

# A Rapid, Non-invasive Method for Anatomical Observations of Tadpole Vertebrae *in Vivo*

Guocheng SHU<sup>1,2</sup>, Shan XIONG<sup>1,2</sup>, Wenyan ZHANG<sup>1,2</sup>, Jianping JIANG<sup>1</sup>, Cheng LI<sup>1\*</sup> and Feng XIE<sup>1\*</sup>

<sup>1</sup> Chengdu Institute of Biology, Chinese Academy of Sciences, Chengdu 610041, China

<sup>2</sup> University of Chinese Academy of Sciences, Beijing 100049, China

**Abstract** The tadpole is a critical stage in the amphibian life cycle and plays an important role during the transition from the aquatic to the terrestrial stage. However, there is a large gap in tadpole research, which represents a vital component of our understanding of the diversity and complexity of the life history traits of amphibians, especially their developmental biology. Some aspects of this gap are due to limited research approaches. To date, X-ray microcomputed tomography (micro-CT) has been widely used to conduct osteology research in adult amphibians and reptiles, but little is known about whether this tool can be applied in tadpole studies. Thus, we compared the results of two methods (the bone-cartilage double-staining technique and micro-CT) to study vertebrae in tadpole specimens. The results revealed no significant difference between the two methods in determining the number of vertebrae, and micro-CT represents a rapid, non-invasive, reliable method of studying tadpole vertebrae. When scanning tadpoles, voltage is the most critical of the scanning parameters (voltage, current and scan time), and moderate scanning parameters are recommended. In addition, micro-CT performed better using specimens stored in 70% ethanol than those preserved in 10% formalin. Finally, we suggest that micro-CT should be more widely applied in herpetological research to increase specimen utilization.

**Keywords** micro-CT, bone-cartilage, double-stain, tadpole, vertebrae

## 1. Introduction

The larval period is an important part of amphibian life history and plays a significant role during the transition from the aquatic to the terrestrial stage. However, at the end of the last century, the tadpoles of approximately two-thirds of the nearly 3 300 known anuran species with a larval phase had not been described (McDiarmid and Altig, 1999), and this knowledge gap is critical to our understanding of the diversity and complexity of

the life history traits of amphibians, especially their developmental biology. Thus, tadpole biology is a discipline within amphibian research that needs to be strengthened. Some aspects of this lack of tadpole research are due to limited methodological approaches.

To obtain an accurate visualization of internal three-dimensional (3D) structures, researchers mainly utilize conventional or modified methods, such as serial histological sectioning (Ročková and Roček, 2005) and gross dissection (Zhang *et al.*, 2016). For example, the bone-cartilage double-staining technique has been widely used in comparative skeletal anatomy studies of small vertebrates since the last century (Hanken and Wassersug, 1981; Simons and Van Horn, 1971; Wassersug, 1976; Williams, 1941), but these methods are typically time-consuming and destructive to the specimens under examination. Recently, non-invasive visualization

\* Corresponding author: Dr. Cheng LI, from Chengdu Institute of Biology, Chinese Academy of Sciences, Chengdu, China, with his research focusing on amphibian taxonomy, tadpole biology and amphibian monitoring. Prof. Feng XIE, from Chengdu Institute of Biology, Chinese Academy of Sciences, Chengdu, China, with his research focusing on histology, ecological adaptation evolution and conservation.

E-mail: licheng@cib.ac.cn (Cheng LI), xiefeng@cib.ac.cn (Feng XIE)

Received: 17 January 2018 Accepted: 14 May 2018

methods have come to the forefront including X-ray microcomputed tomography (micro-CT), which can overcome these weaknesses and visualize the internal anatomy and structural complexity of organisms in the micrometer ( $\mu\text{m}$ ) or nanometer (nm) ranges by relying on differences in the photon attenuation levels of these tissue types (Broeckhoven *et al.*, 2017; Chao *et al.*, 2005; du Plessis *et al.*, 2017; Ritman, 2004, 2011). This approach has been applied in biomedical studies, such as investigations of the skeleton, organs and vascular tree of live mammals, to obtain information on the status or progression of disease (Campbell and Sophocleous, 2014; Ritman, 2004). Micro-CT also provides detailed anatomical interpretations to inform developmental, systematic, and functional morphological research in invertebrates and vertebrates (Gignac *et al.*, 2016; Porro and Richards, 2017; Scherrer *et al.*, 2017). Applications include species identification (Boistel *et al.*, 2011; Faulwetter *et al.*, 2013; Parapar *et al.*, 2017; Scherz *et al.*, 2014) and exploring ecological or evolutionary questions in certain taxa (Broeckhoven and du Plessis, 2017). In herpetology, this tool has been widely used to conduct research in adult amphibians and reptiles (Chen *et al.*, 2012; Fortuny *et al.*, 2015; Kim *et al.*, 2017; Lauridsen *et al.*, 2011; Scherz *et al.*, 2015; Vasquez *et al.*, 2008), but non-invasive micro-CT has not yet been integrated into studies of the developmental biology and osteology of tadpoles. Therefore, we report the use of micro-CT for examining the structure of tadpole vertebrae with the hope of making this modern tool more accessible to the broadest range of morphological researchers across the widest range of fields.

The aims of this study are to 1) investigate the feasibility of micro-CT to examine the structure of tadpole vertebrae *in vivo*, 2) compare the merits and defects of micro-CT with those of conventional methods (bone-cartilage double-staining) in the study of tadpole vertebrae, 3) determine the effects of scanning parameters on image quality, and 4) recommend guidelines for the use of micro-CT in the anatomical study of tadpole vertebrae.

## 2. Materials and Methods

**2.1. Sample preparation** We used 53 tadpole specimens representing three anuran amphibian species from three genera of Megophryidae (Table S1) that were preserved at the Herpetological Museum of the Chengdu Institute of Biology (CIB), CAS. Specimens were first fixed in 10% formalin and then transferred to neutral buffered 10%

formalin (20 individuals) or 70% ethanol (33 individuals) prior to scanning (Table S1). We staged the tadpoles based on the approach of Gosner (1960).

**2.2. Micro-CT scanning** A Quantum GX micro-CT Imaging System (PerkinElmer Health Sciences, USA) was used to acquire high-resolution 3D images of tadpole vertebral structure, located at the Chengdu Institute of Biology (Chengdu, China); this imaging system uses a cone beam X-ray source and a flat-panel X-ray detector to produce high-resolution 3D images of bone structures and the surrounding soft tissues ([www.PerkinElmer.com](http://www.PerkinElmer.com)). To prevent the specimens from drying during scanning, all samples were transferred into 2-ml polypropylene pipette tips (tube's choosing was based on the tadpole size) with 10% formalin or 70% ethanol and then fastened to the sample bed for scanning. In the high-resolution mode, we chose a 72-mm acquisition field of view (FOV) and a 45-mm reconstruction FOV, which allowed for a 9- $\mu\text{m}$  voxel size resolution under a small region (subvolume) reconstruction ([www.PerkinElmer.com](http://www.PerkinElmer.com)). When we compared the results of the two methods (micro-CT scan and double-staining), scanning was conducted for 4 min at a voltage of 70 kV and a current of 80  $\mu\text{A}$ , which produced 458 projection images for every specimen. To detect the effects of scanning parameters (including voltage, current and scan time), we set different levels for each parameter according to the instrument design. Voltage levels were set at 30 kV, 50 kV, 70 kV or 90 kV; current levels were set at 20  $\mu\text{A}$ , 40  $\mu\text{A}$ , 60  $\mu\text{A}$  or 80  $\mu\text{A}$ ; and scan times were set at 8 s, 18 s, 2 min, 4 min, 14 min and 57 min. Skeletal images were reconstructed using these projection images under the Quantum GX micro-CT Imaging System, and surface meshes of the skeleton were produced by regulating the threshold in the volume rendering control panel, which controlled voxel intensity in the 3D reconstruction. The images were exported in BMP (1024  $\times$  1024 pixels) and AVI formats.

**2.3. Bone-cartilage double-staining** Post-scanning, 32 of the 53 scanned specimens (Table S1) were eviscerated and then cleared and stained with alcian blue and alizarin red following the protocol of Hanken and Wassersug (1981).

**2.4. Statistical analysis** The data set was tested for normality prior to analysis, and the Wilcoxon Signed-Rank test was applied to test for inter-method variations (micro-CT and bone-cartilage double-staining) in the determination of the number of tadpole vertebrae. Statistical tests were performed using R software 3.4.2 (R Development Core Team, 2017).

### 3. Results

**3.1. Comparison between micro-CT and bone-cartilage double-staining** The results showed that the two methods (micro-CT and bone-cartilage double-staining) could both clearly display the tadpole vertebrae in the sampled species and that there were no significant differences in the detected number of vertebrae of the tadpoles of the three species (Table 1, Figure 1). The bones were stained purplish red and the cartilage was stained dark blue (Figure 1A, 1C, 1E, 1G, 1I, 1K, 1M, 1O, 1Q and 1S), and after staining, more than half of the tadpoles were bent. Additionally, the bone staining was darker with advancement in developmental stage, especially in the bones (Figure 1 from K to S). The micro-CT could both visualize the bone and discriminate the incompletely ossified cartilage from other tissues (Figure 1 from B to J and from L to T), and the specimens remained in their original positions after scanning. However, the micro-CT seemed unable to distinguish the cartilage located in the head or arthrosis (Figure 1I, 1J, 1S and 1T).

The quality of the CT image differed with the developmental stages of the tadpoles, with the rendering quality of the vertebrae improving with development stage. For example, the images of the vertebrae of the tadpoles at stage 40 were more complete and clearer than those at stage 27 (Figure 1B and 1J). Nevertheless, the results of the double-staining technique showed little association with developmental stage (Figure 1A, 1C and 1I).

We also found that the degree of ossification of vertebrae varied with development stages within species and differed in species at the same stage. Normally, the later development stage is always with the higher degree of ossification within the species. That is, the bony staining color is redder in the higher degree of ossification of vertebrae in this study (Figure 1 from K to S). However, this trend seemed to be not true among species. For example, the degree of ossification of vertebrae in *X. sangzhiensis* was higher than that in *B. carinensis* at the same developmental stage (Figure 1C and 1M), and even the degree of ossification of vertebrae in *X. sangzhiensis* at an early development stage was higher than that of *B. carinensis* at a later development stage (Figure 1C and 1K). Similarly, the number of vertebrae changed with developmental stages. In general, the number of vertebrae increased first and then decreased within species (Figure 1 from L to K). However, there was a large variation among species, for instance, the number of vertebrae of *X. sangzhiensis* was more than that of *B. carinensis* at the

same developmental stage (Figure 1D and 1N).

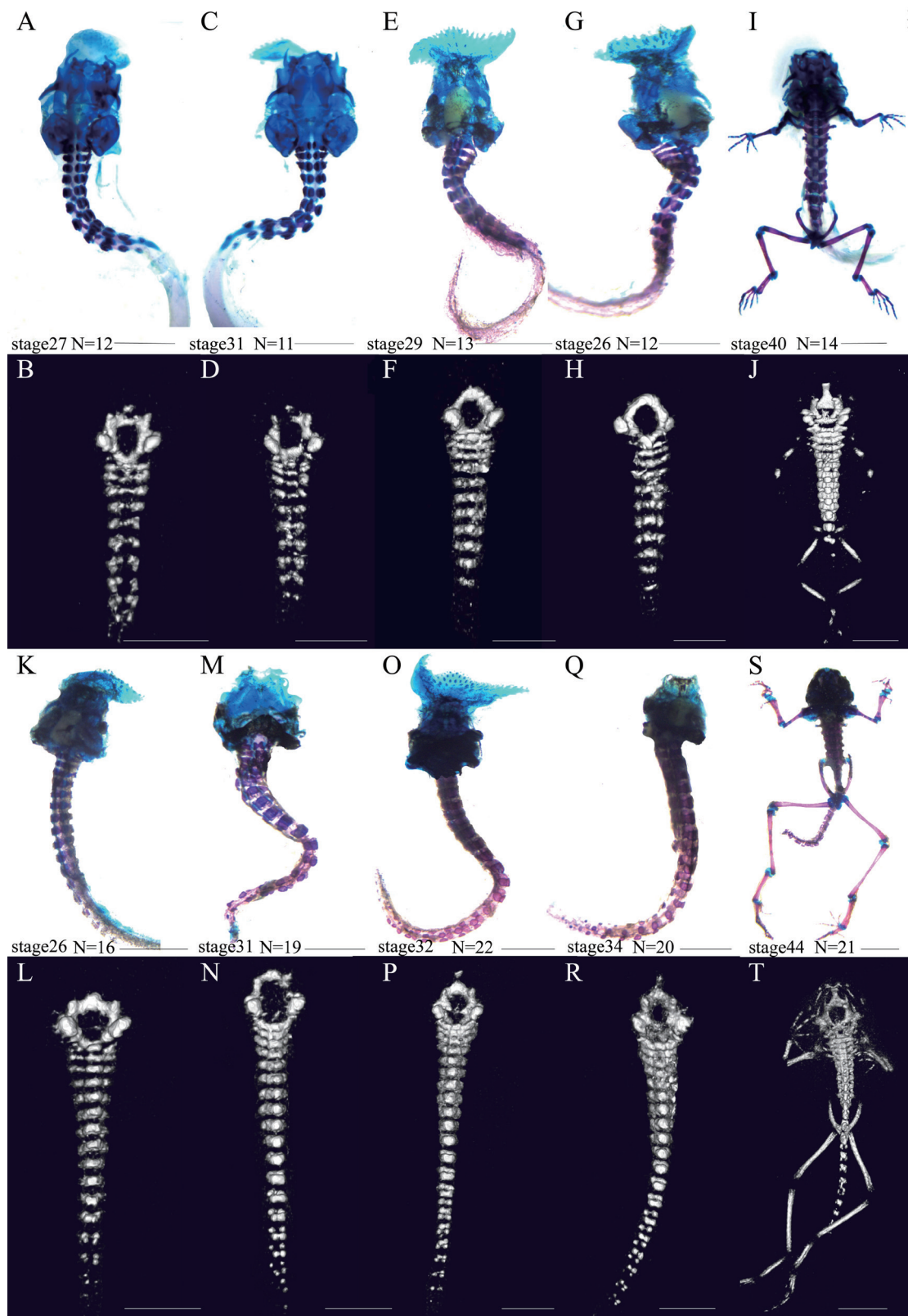
In addition, it was easy to obtain clear 3D images of a tadpole skeleton using micro-CT, such as the three directional views of the vertebrae of the *X. sangzhiensis* tadpole and to acquire detailed information about the vertebrae without destroying the specimens (Figure 2).

**3.2. Factors affecting image quality** We found that the voltage, current and scan time affected image quality. Generally, the image quality increased with increasing voltage (Figure 3A). For instance, at 30 kV, the micro-CT could not distinguish the vertebrae from polypropylene pipette tips (Figure 3, AI and A1), but at 70 kV, the vertebrae of the tadpole were clearly displayed. At 90 kV, the details of the vertebrae could be observed, but it was not possible to differentiate the vertebrae from ethanol (the CT values of the two objects were similar) (Figure 3, AIV and A4). Similar results were observed at different currents, but the impact of the current was less than that of the voltage setting. The image quality was similar under different currents when voltage and scan time were consistent (Figure 3B). Additionally, the image quality increased with scan time (from 8 s to 4 min), although the trend seemingly declined at 14 min (Figure 4IV). As shown in the results, the red arrows indicate that the boundaries of the vertebrae were more clearly displayed with increasing scan time (Figure 4 from 1 to 4), but the image quality did not be obviously improved after scanning for 14 min or longer (Figure 4V, 4VI, 4-5, 4-6).

But beyond that, a stark difference in image quality was revealed between the two preservation methods (70% ethanol or 10% formalin); the image was sharper when the specimens were preserved in 70% ethanol (Figure 5). Furthermore, micro-CT could hardly discern the skulls of tadpoles preserved in formalin, suggesting that preservation has an important effect on scan image quality.

### 4. Discussion

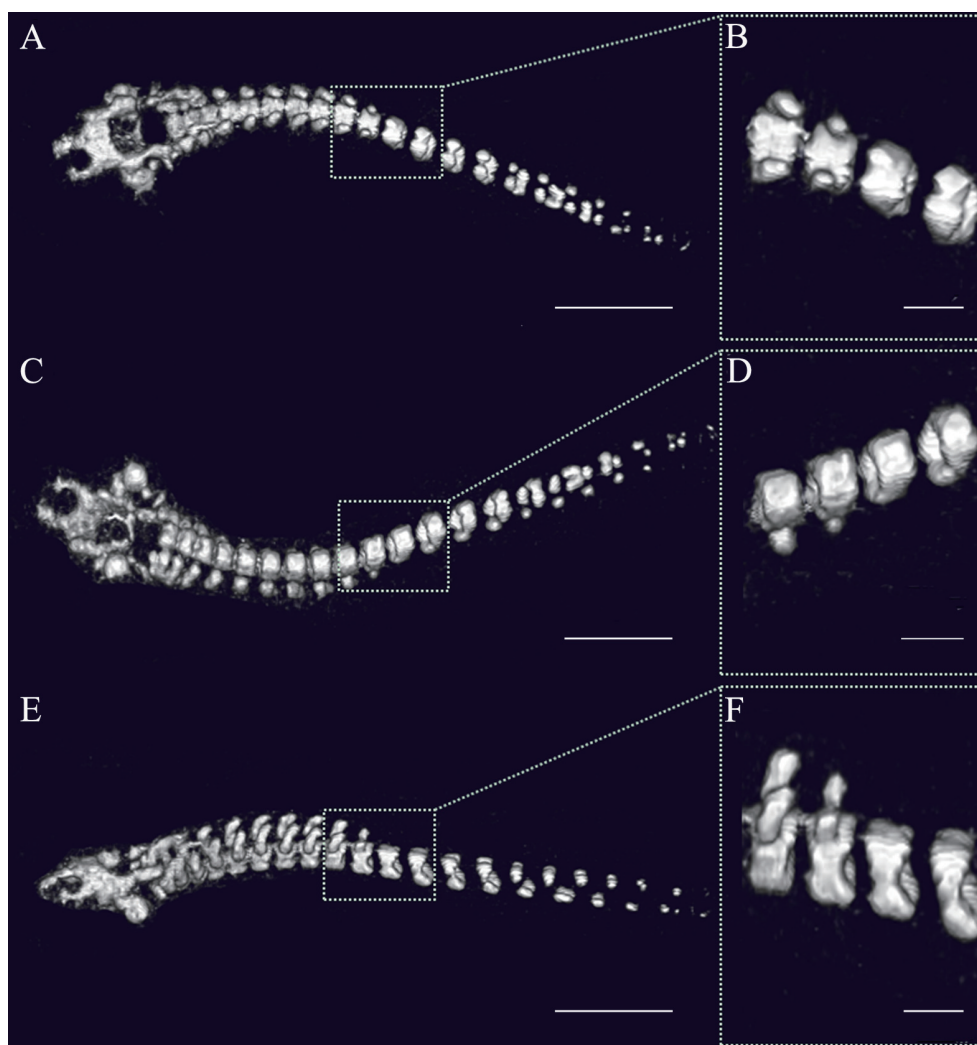
The tadpole skeleton consists of cartilage and bone, but the cartilage accounts for a larger portion during metamorphosis (McDiarmid and Altig, 1999). During this stage, the vertebrae are primarily composed of cartilage with little or no calcium, most of which cannot be stained by alizarin red, so alcian blue or other dyes (such as methylene blue and toluidine blue) have been applied in the double-staining procedure to reveal cartilage in the last several decades (Depew, 2014; Dingerkus and Uhler, 1977; Dingerkus, 1981; Hanken and Wassersug, 1981; Kelly and Bryden, 1983; Redfern *et al.*, 2007;



**Figure 1** Comparison of the two methods for displaying tadpole vertebrae. The white backgrounds are the results of bone-cartilage double-staining (upper), and the black backgrounds are the corresponding micro-CT results (lower) for the same specimens. Specimen cartilage was stained dark blue, and bone stained purplish red. All images present ventral views of the tadpoles. N represents the number of vertebrae. A, B, C, D, I and J: the tadpoles of *B. carinensis*; E, F, G and H: the tadpoles of *A. shapingensis*; and from K to T: the tadpoles of *X. sangzhiensis*. Scale bar: 5 mm.

**Table 1** Comparison of the two methods for examining the number of vertebrae in larval megophryids (Wilcoxon Signed-Rank test).

Species	Individuals	Method	Range	Mean $\pm$ SD	Z	P-value
<i>Xenophrys sangzhiensis</i>	18	micro-CT	9–22	17.33 $\pm$ 3.76	-1	0.317
		double-stain	9–22	17.39 $\pm$ 3.81		
<i>Atympanophrys shapingensis</i>	10	micro-CT	9–14	11.40 $\pm$ 2.01	0	1
		double-stain	9–14	11.40 $\pm$ 2.01		
<i>Brachytarsophrys carinensis</i>	4	micro-CT	11–19	14.00 $\pm$ 3.56	0	1
		double-stain	11–19	14.00 $\pm$ 3.56		
Sum of three species	32	micro-CT	9–22	15.03 $\pm$ 4.25	-0.577	0.564
		double-stain	9–22	15.06 $\pm$ 4.30		

**Figure 2** Micro-CT representations of the skeletal anatomy of the *X. sangzhiensis* tadpole (stage 35). A and B: dorsal view of tadpole vertebrae. C and D: ventral view of tadpole vertebrae. E and F: lateral view of tadpole vertebrae. Left-side scale bar: 5 mm. Right-side scale bar: 2 mm.

Wassersug, 1976; Yamada, 1991). However, this most popular and traditional method is destructive and can distort specimens. Our results show that micro-CT can discern the bone and cartilage from other soft tissues and can produce a 3D image of the vertebrae, although it cannot directly distinguish bone from cartilage without

the help of contrast agents. Moreover, it is non-invasive and can allow researchers to reuse specimens for different research purposes, which is especially important for rare species. Obviously, the method provides an alternative approach to study tadpole vertebrae.

In this study, micro-CT seemingly could not render

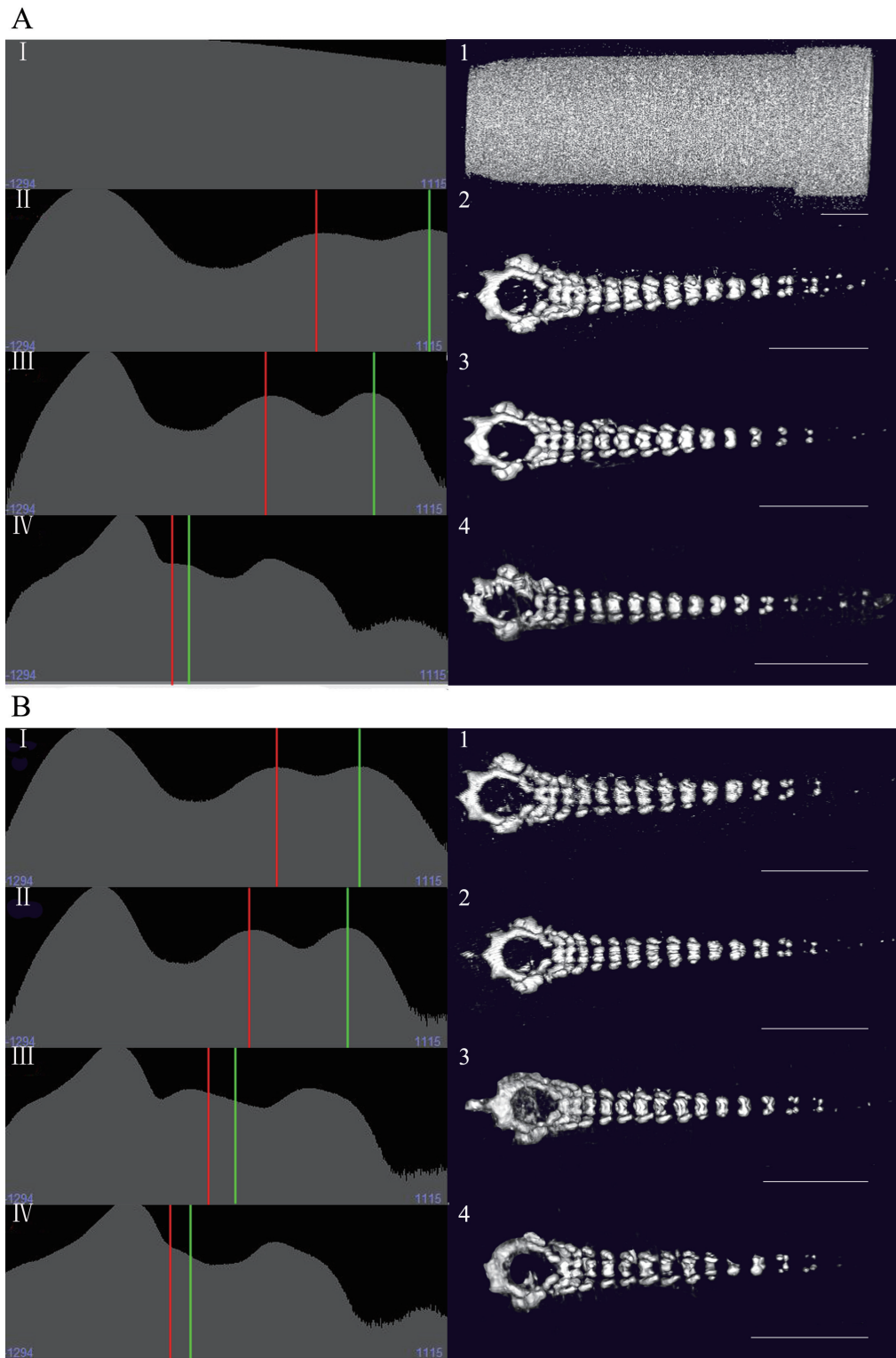


**Figure 3** Renderings of the *X. sangzhiensis* tadpole (stage 34) vertebrae under different scanning voltages or currents. Left histograms (from I to IV) for each parameter show the distributions of voxel values on a relative linear scale. The X-axis represents the CT value (or voxel color table and opacity), and the Y-axis represents the voxel intensity. The ethanol and soft tissues background peak is marked by a solid vertical red line, and the mean of the object voxel distribution is marked by a solid vertical green line. The other peaks represent the voxel distributions of other objects, such as the peak to the left, which represents pore space and air. Images on the right (from 1 to 4) are the scanning results for each parameter. A) The effects of voltage on the scan image. From top to bottom, the respective parameters are 30 kV-88  $\mu$ A-4 min, 50 kV-88  $\mu$ A-4 min, 70 kV-88  $\mu$ A-4 min and 90 kV-88  $\mu$ A-4 min. B) The effects of current on scan image. From 1-4, the respective parameters are 90 kV-20  $\mu$ A-4 min, 90 kV-40  $\mu$ A-4 min, 90 kV-60  $\mu$ A-4 min and 90 kV-80  $\mu$ A-4 min. Scale bar: 5 mm.

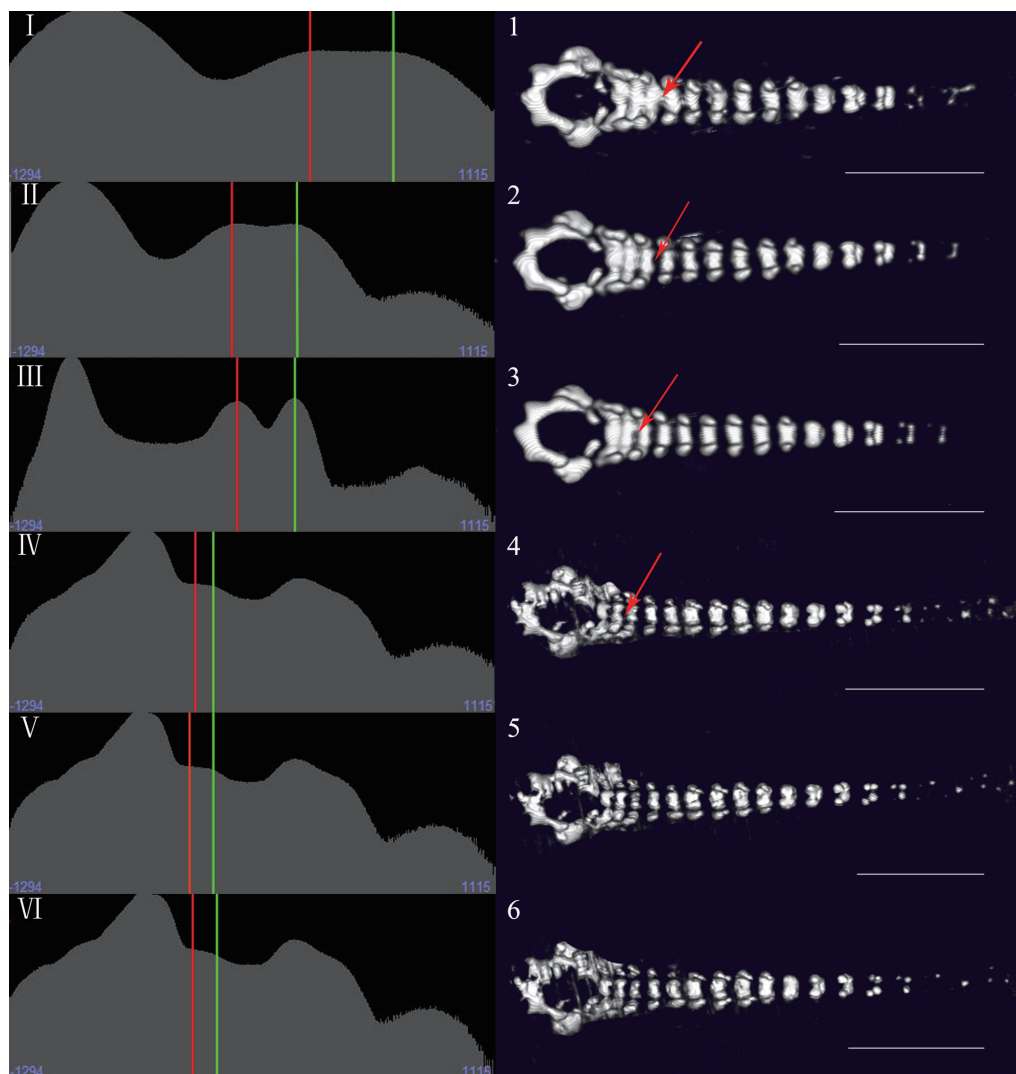


**Figure 4** Renderings of the *X. sangzhiensis* tadpole (stage 34) vertebrae with different scan times. Left histogram (from I to VI) for each parameter shows the distribution of pixel grayscale values on a relative linear scale. The X-axis represents the CT value (or voxel color table and opacity), and the Y-axis represents the voxel intensity. The ethanol and soft tissues background peak is marked by a solid vertical red line, and the mean of the object voxel distribution is marked by a solid vertical green line. The other peaks represent the voxel distributions of other objects, such as the peak on the left, which represents pore space and air. The images on the right are the scanning results for each parameter. The red arrows indicate the boundary between the two vertebrae. From top to bottom, the respective parameters were 90 kV-88  $\mu$ A-8 s, 90 kV-88  $\mu$ A-18 s, 90 kV-88  $\mu$ A-2 min, 90 kV-88  $\mu$ A-4 min, 90 kV-88  $\mu$ A-14 min and 90 kV-88  $\mu$ A-57 min. Scale bar: 5 mm.

cartilage located in the head and appendages, and we speculate that the densities of these cartilages are much less than those of vertebrae due to the lack of calcium. In particular, articular cartilage is mainly composed of proteoglycans, collagens and chondrocytes (Karhula *et al.*, 2017), whose densities are similar to those of other soft tissues, so micro-CT cannot distinguish them. In addition, the main skeleton of the head in a tadpole is chondrocranium which is a cartilaginous case that protects the brain and supports the sense and jaw apparatus (Cannatella, 1999). Based on the results of both double-staining and micro-CT, the skeleton of the

head showed a later ossification time than the vertebrae. In fact, the head has not completely ossified at the end of metamorphosis climax. And, the first sign of appendicular skeletal development usually appears after stage 37 in megophryids (Handrigan *et al.*, 2007). Thus, it is more effective to study the vertebrae than other parts of the skeleton by micro-CT in megophryid tadpole. Furthermore, the scan image quality increases with developmental stage, mainly due to the different degrees of vertebral calcification. Scherz *et al.* (2015) reported that micro-CT scanning can nicely render highly calcified structures, especially bone, because tadpoles have

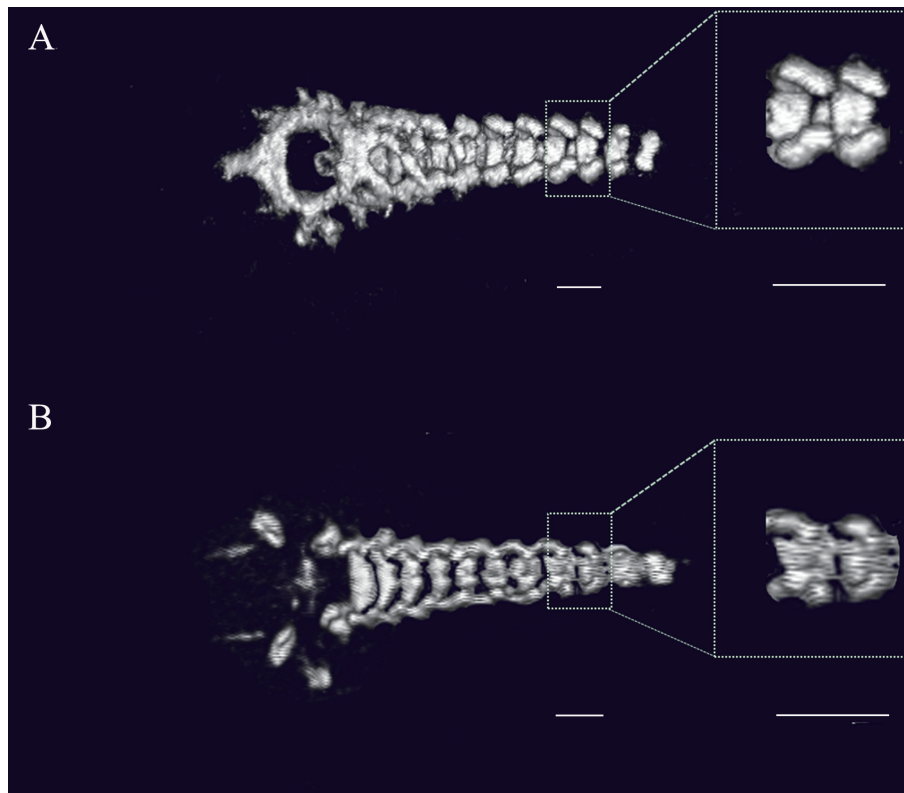


**Figure 5** Scanned images of *A. shapingensis* tadpoles (stage 37) stored in 70% ethanol (A) and in 10% formalin (B). Scale bar: 2 mm.

relatively higher ossification levels at later developmental stages. So, micro-CT scanning is more suitable for tadpoles at later stages.

Indeed, the non-mineralized structures (such as soft tissues) in small vertebrates or invertebrates can also be visualized by micro-CT with the help of contrast agents (Descamps *et al.*, 2014; Gignac *et al.*, 2016; Metscher, 2009a), such as PTA (1% (w/v) phosphotungstic acid in water) and IKI (1% iodine metal (I<sub>2</sub>) + 2% potassium iodide (KI) in water); Some soft tissues of *Xenopus laevis* tadpoles have been successfully studied using micro-CT in combination with a contrast agent (PTA) (Descamps *et al.*, 2014; Metscher, 2009b). Thus, we can also combine with the contrast agent to explore the anatomy and osteology of tadpole when conducting CT scan.

The degree of ossification of vertebrae has drastic variation among species at the same developmental stage. As shown in this study, the degree of ossification of *X. sangzhiensis* at the same or an earlier stage was higher than that in *B. carinensis*. Meanwhile, the number of vertebrae in the former is much more than that in the latter. This difference may be mainly related to the heterochronous arrest of bony development. Trueb (1973) reported that heterochrony is operational in the maintenance of osteological differences between the

sexes in hylids. E. M. T. Stephenson (1960) and N. G. Stephenson (1965) also argued that the heterochronous changes would result in some types of osteological differences among closely related species. Thus, we speculate that the degree of ossification of vertebrae varied with species also resulted from the heterochrony of bony development. Furthermore, axial and appendicular skeletal development usually starts in quick succession and then proceeds together in anurans (Maglia 2003). However, Handrigan *et al.* (2007) found that much of vertebral column development occurred before the onset of ossification in the limbs in megophryids. We also revealed a similar phenomenon that the degree of ossification of vertebrae is different between species at the same developmental stage (or the same development level of the external limb). So, the Gosner staging table that is based primarily on limb development is not always an appropriate standard for all species as megophryid tadpole (Handrigan *et al.*, 2007).

For tadpole scanning, the voltage played a key role among the scanning parameters, but it is inadvisable to choose an overly high or low voltage since these scanning parameters can increase the overlapping intensities between the void and solid phases, which will reduce the degree of differentiation. Similar results were

observed when comparing different currents or scan time, so we recommend moderate scanning parameters (such as 70 kV-80  $\mu$ A-4 min) when scanning tadpoles. In addition, micro-CT performed poorly when using specimens stored in formalin preservative because formalin can decalcify the skeleton, especially bone (Heyer *et al.*, 1994), diminishing the contrast between the skeleton and soft tissues. Therefore, we suggest that specimens to scan should be preserved in 70% ethanol, or formalin preservative should be kept neutral to reduce decalcification.

Bone-cartilage double-staining is a critical tool for evolutionary and developmental biologists to evaluate the ontogeny of the skeleton (Depew, 2009) because it can clearly distinguish differences between bone and cartilage. However, this process is time-consuming and complex, requires specialized chemicals, and is ultimately destructive to the specimens, preventing future uses (Hanken and Wassersug, 1981; Simons and Van Horn, 1971; Wassersug, 1976; Williams, 1941). These issues are especially impactful for rare specimens that must be utilized for a variety of studies, but micro-CT can avoid these drawbacks due to its non-invasive nature. First, we can dissect tadpole vertebrae *in vivo* without damaging the samples, which is very important for preserving rare specimens. Second, it is convenient and efficient to scan a large number of samples. Furthermore, we can reconstruct a particular structure or slice(s) at a higher resolution (du Plessis *et al.*, 2017). It is also possible to repeatedly change the scanning parameters until a satisfactory image is obtained, and the multiple output files (including video format) from micro-CT can be viewed using different software.

## 5. Conclusion

This study demonstrated that micro-CT is a rapid, non-invasive, reliable and efficient method for studying the vertebrae of tadpoles and can increase specimen utilization. Correspondingly, it also provides an alternative approach to study vertebrae in tadpole biology. Ethanol preservative and moderate scanning parameters are recommended in tadpole scan. Furthermore, we suggest that micro-CT, alone or in combination with bone-cartilage double-staining, be more widely applied in herpetological research to promote the development of the field.

**Acknowledgements** The project is supported by the National Key Program of Research and Development,

Ministry of Science and Technology (No. 2017YFC05 05202 granted to Jianping JIANG) and the National Natural Science Foundation of China (No. 31172055 granted to Cheng LI and No. 31172174 granted to Feng XIE). We are grateful to the Herpetological Museum of the Chengdu Institute of Biology for facilitating our examination of the specimens and to Nicholas C. WU for proof reading the manuscript.

## References

- Boistel R., Swoger J., Kržič U., Fernandez V., Gillet B., Reynaud E. G.** 2011. The future of three-dimensional microscopic imaging in marine biology. *Mar Biol*, 32(4): 438–452
- Broeckhoven C., Plessis A., Roux S. G., Mouton P. L. F. N., Hui C.** 2017. Beauty is more than skin deep: A non-invasive protocol for *in vivo* anatomical study using micro-CT. *Methods Ecol Evol*, 8(3): 358–369
- Campbell G. M., Sophocleous A.** 2014. Quantitative analysis of bone and soft tissue by micro-computed tomography: Applications to *ex vivo* and *in vivo* studies. *Bonekey Rep*, 3: 564
- Cannatella D.** 1999. Architecture: Cranial and axial musculoskeleton. In McDiarmid R. W., Altig R. (Eds.), *Tadpoles: the biology of anuran larvae*. Chicago, USA: University of Chicago Press, 52–81
- Chao W., Harteneck B. D., Liddle J. A., Anderson E. H., Attwood D. T.** 2005. Soft X-ray microscopy at a spatial resolution better than 15 nm. *Nature*, 435(7046): 1210–1213
- Chen Y., Lin G., Chen Y., Fok A., Slack J. M.** 2012. Micro-computed tomography for visualizing limb skeletal regeneration in young *Xenopus* frogs. *Anat Rec*, 295(10): 1562–1565
- Depew M. J.** 2009. Analysis of skeletal ontogenesis through differential staining of bone and cartilage. In Westendorf (Eds.), *Molecular Embryology: Methods and Protocols*. Totowa, USA: Humana Press. 37–4
- Descamps E., Buytaert J., De Kegel B., Dirckx J., Adriaens D.** 2012. A qualitative comparison of 3D visualization in *Xenopus laevis* using a traditional method and a non-destructive method. *Belg J Zool*, 142(2): 99–111
- Dingerkus G., Uhler L. D.** 1977. Enzyme clearing of Alcian blue stained whole small vertebrates for demonstration of cartilage. *Stain Technol*, 52: 229–232
- Dingerkus G.** 1981. The use of various alcohols for Alcian blue in toto staining of cartilage. *Stain Technol*, 56: 128–129
- Dodd M. H. I., Dodd J. M.** 1976. The biology of metamorphosis. *Physiol Amphibia*, 3: 467–599
- Du Plessis A., Broeckhoven C., Guelpa A., Le Roux S. G.** 2017. Laboratory X-ray micro-computed tomography: A user guideline for biological samples. *GigaScience*, 6(6): 1–11
- Faulwetter S., Vasileiadou A., Kouratoras M., Dailianis T., Arvanitidis C.** 2013. Micro-computed tomography: Introducing new dimensions to taxonomy. *ZooKeys*, 263: 1
- Fortuny J., Marcé-Nogué J., Heiss E., Sanchez M., Gil L., Galobart À.** 2015. 3D bite modeling and feeding mechanics of the largest living amphibian, the Chinese giant salamander *Andrias davidianus* (Amphibia: Urodela). *PLoS One*, 10(4):

e0121885

- Gignac P. M., Kley N. J., Clarke J. A., Colbert M. W., Morhardt A. C., Cerio D., Cost I. N., Cox P. G., Daza J. D., Early C. M., Echols M. S., Henkelman R. M., Herdina A. N., Holliday C. M., Li Z., Mahlow K., Merchant S., Müller J., Orsbon C. P., Paluh D. J., Thies M. L., Tsai H. P., Echols M. S.** 2016. Diffusible iodine based contrast enhanced computed tomography (diceCT): An emerging tool for rapid, high resolution, 3D imaging of metazoan soft tissues. *J Anat*, 228(6): 889–909
- Gosner K. L.** 1960. A simplified table for staging anuran embryos and larvae with notes on identification. *Herpetologica*, 16(3): 183–190
- Handrigan G. R., Haas A., Wassersug R. J.** 2007. Bony-tailed tadpoles: The development of supernumerary caudal vertebrae in larval megophryids (Anura). *Evol Dev*, 9(2): 190–202
- Hanken J., Wassersug R.** 1981. The visible skeleton. *Funct Photo*, 16(4): 22–26
- Heyer R., Donnelly M. A., Foster M., McDiarmid R.** 1994. Measuring and monitoring biological diversity: Standard methods for amphibians. Washington, USA: Smithsonian Institution Press. 289–297
- Karhula S. S., Finnilä M. A., Lammi M. J., Ylärinne J. H., Kauppinen S., Rieppo L., Pritzker K. P. H., Nieminen H. J., Saarakkala S.** 2017. Effects of articular cartilage constituents on phosphotungstic acid enhanced micro-computed tomography. *PLoS One*, 12(1): e0171075
- Kelly W. L., Bryden M. M.** 1983. A modified differential stain for cartilage and bone in whole mount preparations of mammalian fetuses and small vertebrates. *Stain Technol*, 58:131–134
- Kim E., Sung H., Lee D., Kim G., Nam D., Kim E.** 2017. Nondestructive skeletal imaging of *Hyla suweonensis* using Micro-computed tomography. *Asian Herpetol Res*, 88(4): 235–243
- Lauridsen H., Hansen K., Wang T., Agger P., Andersen J. L., Knudsen P. S., Maglia, A. M.** 2003. Skeletal development of *Pelobates cultripes* and comparisons of the osteology of pelobatoid frogs. *Sci Pap Univ Kansas Nat Hist Mus*, 30: 1–13
- McDiarmid R. W., Altig R.** 1999. Tadpoles: the biology of anuran larvae. Chicago, USA: University of Chicago Press. 52–90
- Metscher B. D.** 2009a. MicroCT for developmental biology: A versatile tool for high-contrast 3D imaging at histological resolutions. *Dev Dyn*, 238(3): 632–640
- Metscher B. D.** 2009b. MicroCT for comparative morphology: simple staining methods allow high-contrast 3D imaging of diverse non-mineralized animal tissues. *BMC Physio*, 9(1): 11
- Mizutani R., Suzuki Y.** 2012. X-ray microtomography in biology. *Micron*, 43(2): 104–115
- Parapar J., Candás M., Cunha-Veira X., Moreira J.** 2017. Exploring annelid anatomy using micro-computed tomography: A taxonomic approach. *Zool Anz*, 270: 19–42
- Porro L. B., Richards C. T.** 2017. Digital dissection of the model organism *Xenopus laevis* using contrast-enhanced computed tomography. *J Anat*, 231: 169–191
- Rasmussen A. S., Uhrenholt L., Pedersen M.** 2011. Inside out: modern imaging techniques to reveal animal anatomy. *PLoS One*, 6(3): e17879
- Redfern B. G., David W. L., Spence S.** 2007. An alternative Alcian blue dye variant for the evaluation of fetal cartilage. *Birth Defects Res B*, 80(3): 171–176
- Ritman E. L.** 2004. Micro-computed tomography—current status and developments. *Annu Rev Biomed Eng*, 6: 185–208
- Ritman E. L.** 2011. Current status of developments and applications of micro-CT. *Annu Rev Biomed Eng*, 13: 531–552
- Ročková H., Roček Z.** 2005. Development of the pelvis and posterior part of the vertebral column in the Anura. *J Anat*, 206(1): 17–35
- R Development Core Team.** 2017. R: A language and environment for statistical computing. R Foundation for Statistical Computing, Vienna, Austria. Available from: <http://www.R-project.org> (accessed 28 September 2017).
- Scherrer R., Hurtado A., Machado E. G., Debais-Thibaud M.** 2017. MicroCT survey of larval skeletal mineralization in the Cuban gar *Atractosteus tristoechus* (Actinopterygii; Lepisosteiformes). *MorphoMuseum*, 3(3):e3
- Scherz M. D., Ruthensteiner B., Vences M., Glaw F.** 2014. A new microhylid frog, genus *Rhombophryne*, from northeastern Madagascar, and a re-description of *R. serratopalpebrosa* using micro-computed tomography. *Zootaxa*, 3860(6): 547–560
- Scherz M. D., Ruthensteiner B., Vieites D. R., Vences M., Glaw F.** 2015. Two new microhylid frogs of the genus *Rhombophryne* with superciliary spines from the Tsaratanana Massif in northern Madagascar. *Herpetologica*, 71(4): 310–321
- Sephenson M. T.** 1960. The skeletal characters of *Leiopelma hamiltoni* McCulloch, with particular reference to the effects of heterochrony on the genus. *Trans Roy Soc*, 88 (3): 473–488
- Sephenson N. G.** 1965. Heterochronous changes among Australian leptodactylid frogs. *Proc Zool Soc*, 144 (3): 339–350
- Simons E. V., Van Horn J. R.** 1971. A new procedure for whole-mount Alcian blue staining of the cartilaginous skeleton of chicken embryos, adapted to the clearing procedure in potassium hydroxide. *Acta Morphol Neerl-Scand*, 8: 281–292
- Trueb L.** 1973. Bones, frogs, and evolution. In Vial J. L. (Eds.) *Evolutionary biology of anurans*. Columbia: University of Missouri Press, 65–132
- Vasquez S. X., Hansen M. S., Bahadur A. N., Hockin M. F., Kindlmann G. L., Nevell L., Isabel Q. Wu., David J. G., David M. W., Greg M. J., Christopher R. J., John L. V., Mario R. C., Johnson C. R.** 2008. Optimization of volumetric computed tomography for skeletal analysis of model genetic organisms. *Anat Rec*. 291(5): 475–487
- Wassersug R. J.** 1976. A procedure for differential staining of cartilage and bone in whole formalin-fixed vertebrates. *Stain Technol*, 51(2): 131–134
- Williams T. W.** 1941. Alizarin red S and toluidine blue for differentiating adult or embryonic bone and cartilage. *Stain Technol*, 16: 23–25
- Yamada T.** 1991. Selective staining methods for cartilage of rat fetal specimens previously treated with alizarin red S. *Teratology*, 43(6): 615–619
- Zhang M., Chen X., Chen X.** 2016. Osteology of *Quasipaa robertingeri* (Anura: Dicroglossidae). *Asian Herpetol Res*, 7(4): 242–250

## Appendix

**Table S1** Information on the samples used in this study.

Species	Catalogue	Gosner stage	Preservation	Processing
<i>Atympanophrys shapingensis</i>	LZPHST01	27	70% ethanol	CTS&DS
<i>Atympanophrys shapingensis</i>	LZPHST02	28	70% ethanol	CTS&DS
<i>Atympanophrys shapingensis</i>	131555-03	26	70% ethanol	CTS&DS
<i>Atympanophrys shapingensis</i>	131555-04	28	70% ethanol	CTS&DS
<i>Atympanophrys shapingensis</i>	131555-06	29	70% ethanol	CTS&DS
<i>Atympanophrys shapingensis</i>	131555-08	30	70% ethanol	CTS&DS
<i>Atympanophrys shapingensis</i>	LZP201606-01	37	70% ethanol	CTS&DS
<i>Atympanophrys shapingensis</i>	LZP201606-02	25	70% ethanol	CTS&DS
<i>Atympanophrys shapingensis</i>	LZP20160418	31	70% ethanol	CTS&DS
<i>Atympanophrys shapingensis</i>	LZP2015101201-01	27	70% ethanol	CTS&DS
<i>Atympanophrys shapingensis</i>	K0034-01	27	10% formalin	CTS
<i>Atympanophrys shapingensis</i>	K0034-02	28	10% formalin	CTS
<i>Atympanophrys shapingensis</i>	K0034-03	26	10% formalin	CTS
<i>Atympanophrys shapingensis</i>	K0034-04	27	10% formalin	CTS
<i>Atympanophrys shapingensis</i>	K0034-05	38	10% formalin	CTS
<i>Atympanophrys shapingensis</i>	K0034-06	39	10% formalin	CTS
<i>Atympanophrys shapingensis</i>	K0034-07	37	10% formalin	CTS
<i>Atympanophrys shapingensis</i>	K0034-08	36	10% formalin	CTS
<i>Xenophrys sangzhiensis</i>	TPS57	34	70% ethanol	CTS
<i>Xenophrys sangzhiensis</i>	TPS01	27	70% ethanol	CTS&DS
<i>Xenophrys sangzhiensis</i>	TPS02	32	70% ethanol	CTS&DS
<i>Xenophrys sangzhiensis</i>	TPS03	33	70% ethanol	CTS&DS
<i>Xenophrys sangzhiensis</i>	TPS04	26	70% ethanol	CTS&DS
<i>Xenophrys sangzhiensis</i>	TPS06	37	70% ethanol	CTS&DS
<i>Xenophrys sangzhiensis</i>	TPS08	35	70% ethanol	CTS&DS
<i>Xenophrys sangzhiensis</i>	TPS10	25	70% ethanol	CTS&DS
<i>Xenophrys sangzhiensis</i>	TPS29	26	70% ethanol	CTS&DS
<i>Xenophrys sangzhiensis</i>	TPS30	32	70% ethanol	CTS&DS
<i>Xenophrys sangzhiensis</i>	TPS32	34	70% ethanol	CTS&DS
<i>Xenophrys sangzhiensis</i>	TPS35	42	70% ethanol	CTS&DS
<i>Xenophrys sangzhiensis</i>	TPS36	32	70% ethanol	CTS&DS
<i>Xenophrys sangzhiensis</i>	TPS37	44	70% ethanol	CTS&DS
<i>Xenophrys sangzhiensis</i>	TPS45	34	70% ethanol	CTS&DS
<i>Xenophrys sangzhiensis</i>	TPS53	31	70% ethanol	CTS&DS
<i>Xenophrys sangzhiensis</i>	TPS89	30	70% ethanol	CTS&DS
<i>Xenophrys sangzhiensis</i>	TPS98	29	70% ethanol	CTS&DS
<i>Xenophrys sangzhiensis</i>	2015102101-07	36	70% ethanol	CTS&DS
<i>Brachytarsophrys carinensis</i>	3655	35	70% ethanol	CTS&DS
<i>Brachytarsophrys carinensis</i>	3823-01	40	70% ethanol	CTS&DS
<i>Brachytarsophrys carinensis</i>	3823-02	27	70% ethanol	CTS&DS
<i>Brachytarsophrys carinensis</i>	3823-03	31	70% ethanol	CTS&DS
<i>Brachytarsophrys carinensis</i>	150143-01	26	10% formalin	CTS
<i>Brachytarsophrys carinensis</i>	150143-02	26	10% formalin	CTS
<i>Brachytarsophrys carinensis</i>	150143-03	26	10% formalin	CTS
<i>Brachytarsophrys carinensis</i>	150143-04	26	10% formalin	CTS
<i>Brachytarsophrys carinensis</i>	150143-05	26	10% formalin	CTS
<i>Brachytarsophrys carinensis</i>	150143-06	26	10% formalin	CTS
<i>Brachytarsophrys carinensis</i>	150143-07	26	10% formalin	CTS
<i>Brachytarsophrys carinensis</i>	150143-08	26	10% formalin	CTS
<i>Brachytarsophrys carinensis</i>	150143-09	26	10% formalin	CTS
<i>Brachytarsophrys carinensis</i>	150143-10	26	10% formalin	CTS
<i>Brachytarsophrys carinensis</i>	150143-11	26	10% formalin	CTS
<i>Brachytarsophrys carinensis</i>	150143-12	26	10% formalin	CTS

CTS: CT scan, DS: Double stain